

Enhancing the Porosity of Mesoporous Carbon-Templated ZSM-5 by Desilication

Martin S. Holm,^[a,b] Kresten Egeblad,^[a] Peter N. R. Vennestrom,^[a] Christian G. Hartmann,^[a] Marina Kustova,^[b] and Claus H. Christensen^{*[b]}

Keywords: ZSM-5 / Zeolites / Desilication / Carbon-templating / Mesoporous materials

A tunable desilication protocol applied on a mesoporous ZSM-5 zeolite synthesized by carbon-templating is reported. The strategy enables a systematic manufacture of zeolite catalysts with moderate to very high mesoporosities. Coupling carbon-templating and desilication thus allow for more than a doubling of the original mesopore volume and mesopore surface area. The porosity effect arising from various treatment times and base amounts in the media has been

thoroughly mapped. Initially, small mesopores are created, and as desilication strength increases the average mesopore size enhances. Crystallinity of the treated samples is retained, and electron microscopy indicates solely intracrystalline mesoporosity.

(© Wiley-VCH Verlag GmbH & Co. KGaA, 69451 Weinheim, Germany, 2008)

Introduction

Zeolites are crystalline microporous aluminosilicates that have found a multitude of industrial applications as, e.g. sorbents, ion-exchangers, and catalysts. The widespread application of zeolites in industry can be attributed to the inherent micropore system of molecular dimensions, which allows for shape-selective catalysis. Moreover, they are often thermally highly stable materials, which possess remarkably high surface areas. These properties make zeolites particularly useful for catalytic applications, and the use of zeolites as catalysts has indeed received significant attention.^[1,2] However, molecular transport to the catalytically active micropore system in the bulk of the crystals may become a limiting factor for their activity in some catalytic applications.^[3] Recently, several preparative strategies have been developed with the aim of producing zeolite materials that overcome this diffusion limitation.^[4,5] The strategies pursued so far include increasing the width of the zeolite micropores,^[6–9] decreasing the size of the zeolite crystals,^[10–14] and the introduction of an auxiliary mesopore system in addition to the inherent micropore system.^[15–18] The latter two classes of materials can be classified as hierarchical in terms of porosity because they have bi- or trimodal pore-size distributions, and the preparation of such materials by use of mesopore templates was reviewed very

recently.^[19] For the preparation of zeolites with intracrystalline hierarchical porosity, two main approaches appear to be the most promising,^[20] namely carbon-templating^[21–23] and desilication.^[24–27]

In carbon-templating, porous zeolite crystals are produced by removal of auxiliary carbon particles encapsulated in the zeolite crystals during growth. In desilication, conventional purely microporous zeolite crystals are treated with dilute aqueous base to preferentially dissolve silica species from the zeolite crystals. Here, we show that the porosity of carbon-templated mesoporous zeolite crystals can be tuned, as well as increased by more than a factor of two, by subjecting the already mesoporous material to a desilication procedure. Coupling of these two procedures have in fact been attempted earlier, however, with limited success.^[28] The process of desilication corresponds to a partial dissolution of the zeolite framework. Therefore, it is important either to use a limited amount of a base or to restrict the time during which the process is allowed to proceed.^[29]

Results and Discussion

A mesoporous carbon-templated ZSM-5 zeolite was subjected to various desilication treatments as listed in Table 1.

Physico-chemical properties of the resulting materials from N₂ physisorption, XRD and NH₃-TPD measurements are included. First of all, it can be seen that the microporosity is preserved after desilication since the micropore volumes of the samples are not affected by the treatments. Moreover, it can be seen that the parent carbon-templated sample has a considerable mesopore volume of ca. 0.3 mL/g.

[a] Center for Sustainable and Green Chemistry, Department of Chemistry, Technical University of Denmark, Building 206, 2800 Lyngby, Denmark

[b] Haldor Topsoe A/S, Nymøllevej 55, 2800 Lyngby, Denmark
E-mail: chc@topsoe.dk

Supporting information for this article is available on the WWW under <http://www.eurjic.org> or from the author.

Table 1. Textural data from N₂ adsorption/desorption experiments on the parent and desilicated samples.^[a]

Sample	Base amount [mmol/g]	Time [min]	S_{BET} [m ² /g]	S_{meso} [m ² /g]	V_{meso} [mL/g]	V_{micro} [mL/g]	$D[101]^{\text{[b]}}$ [Å]	Acidity ^[c] [mmol/g]
Parent	—	—	408	117	0.30	0.11	677	0.164
1	3	30	408	162	0.37	0.11	595	0.180
2	5	30	422	195	0.47	0.10	513	0.206
3	7.5	30	478	222	0.63	0.11	494	0.235
4	10	30	478	232	0.72	0.10	460	0.272
5	15	30	503	234	0.75	0.11	386	0.293
6	8	5	295	142	0.33	0.06	—	—
7	8	10	466	241	0.64	0.10	—	—
8	8	15	443	210	0.66	0.10	—	—
9	8	20	456	208	0.70	0.11	—	—
10	8	30	450	201	0.73	0.11	—	—
11	8	70	445	181	0.65	0.11	—	—

[a] Samples 1–5 were desilicated in a 0.1 M solution and samples 6–11 in a 0.2 M solution. $V_{\text{meso}} = V_{\text{ads}, P/P_0 = 0.99} - V_{\text{micro}}$. V_{micro} from t -plot. S_{meso} from BJH. Surface area of pores 17–3000 Å. [b] Scherrer equation. [c] NH₃-TPD. NH₃ desorbed at 175 °C for 2 h.

This porosity corresponds to a moderate mesopore surface area S_{meso} of 117 m²/g due to rather large mesopores centered around ca. 20–30 nm. The physisorption isotherms obtained from samples treated with different volumes of 0.1 M NaOH solutions for 30 min (samples 1–5) are shown in Figure 1(a). In Figure 1(a) it can be seen that the mesopore volume of the samples increases with increasing desilication strength. Moreover, closer inspection of Figure 1(a) reveals that a hysteresis loop starts to develop at a relative pressure of 0.45 at low treatment strengths (samples 1 and 2). This is attributed to the formation of new smaller mesopores, initially with a diameter below 10 nm as is evident from the BJH-derived pore-size distribution given in Figure 1(b).

The sizes of the created mesopores are in excellent agreement with previously published data on desilication of purely microporous ZSM-5 samples.^[30,31] Interestingly, because the mesopores initially formed are smaller than the inherent mesopore system present, these results indicate that it is possible to create a hierarchical zeolite with a multi-level mesoporosity by coupling the carbon-templating and desilication protocols. As the desilication strength is increased, these smaller mesopores grow larger, as can be seen by the disappearance of the mesopores below 10 nm (samples 3 and 4) and simultaneous growth of pore volume attributed to pores around 15 nm. Thus, the observed increase in mesopore volumes apparent from Table 1 does not only originate from an increase in the pore sizes of already existing mesopores, but also from newly generated mesopores. The generation of mesopores can also be tuned by variation of the reaction time as evident from the physisorption data presented in Table 1 for samples 6–11. It can be seen, that the mesopore volume as well as the mesopore surface area of the parent mesoporous sample are doubled after only 10 min (sample 7). Moreover, it can be seen that further extending the desilication time only marginally increases the mesopore volume, and an extreme time has a detrimental effect on the mesopore surface area (sample 11). This is attributed to the pore size distribution extending significantly into the macropore region. Key sorp-

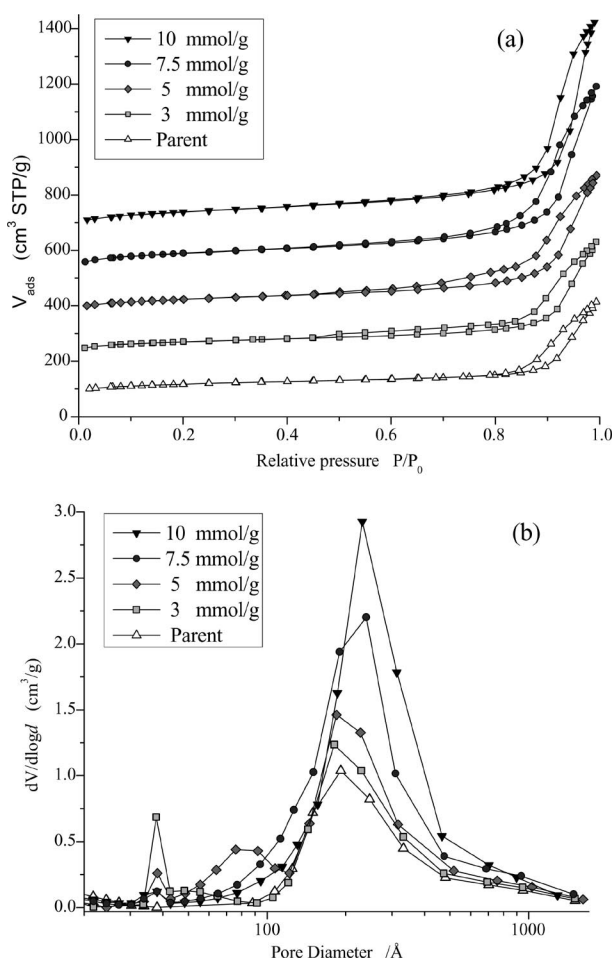


Figure 1. (a) N₂ adsorption/desorption isotherms of the parent along with samples 1–4. Isotherms of samples 1–4 are offset by 150 for illustrative reasons. (b) BJH-derived pore-size distributions.

tion isotherms and the respective BJH-derived mesopore diameters are given in the Supporting Information (Figure S1). Figure 2 shows the XRD patterns of the parent sample along with samples 1–5 illustrating the preserved crystallinity and phase purity of the treated samples. In ac-

cordance with results obtained after desilication of conventional zeolite samples, the intensity of the reflections gradually decrease as the desilication strength is increased.^[32,33]

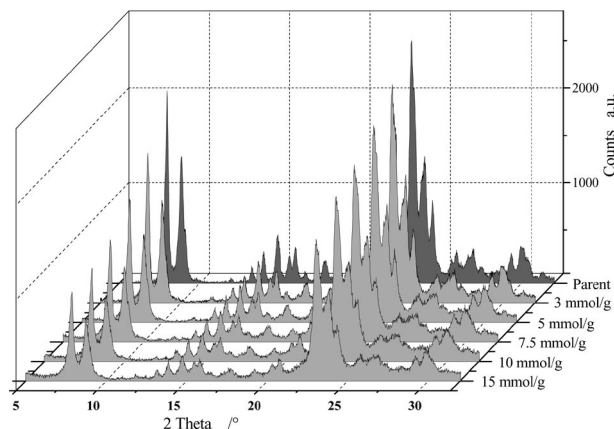


Figure 2. XRD diffractograms of parent sample and samples 1–5 desilicated for 30 min with increasing desilication strength.

The effective average crystal diameter calculated by the Scherrer equation reveal a gradual decrease in crystal diameter. The D[101] deflection was chosen for Table 1. Table S1 (Supporting Information) contains effective crystal sizes derived from other deflections. By analyzing the XRD results in relation to imaging obtained from SEM and TEM analysis, it appears unlikely that the desilicated crystals dismantle to produce interparticle mesoporosity. The observed decrease in the average crystal size could alternatively be explained by the formation of an increasing number of intracrystalline domains bordering a mesopore within the single crystal. From NH_3 -TPD an acidity of 0.164 mmol/g was measured for the parent sample after desorption of NH_3 at 175 °C for 2 h. This acidity correlates to the anticipated Si/Al ratio of approximately 45 when compared to a calibration curve from ZSM-5 zeolites of known acidities, thus indicating complete aluminium incorporation from the gel during crystallization. Furthermore, it can be seen from Table 1 (samples 1–5) that the total acidity of the materials increase as a function of the desilication, as would be expected from the selective silicon extraction. Figure 3 presents the NH_3 desorption curves obtained after desorption of weakly bound NH_3 at 100 °C for 1 h and at 175 °C for 2 h. A continuing increase in total acidity and nearly a doubling for the most severely treated zeolites is apparent in both cases. In Figure 3(b) it can be seen that a significant contribution to the acidity originates from a shoulder on the low-temperature side of the desorption maximum at ca. 365 °C. As the treatment strength increases, the shoulder intensifies, which is possibly due to partial (extra) framework aluminum species generated during the desilication.

Figure 4 gives representative SEM and TEM images of the parent and desilicated samples. SEM was used to verify the homogeneity of the parent material with respect to crystal size and porosity, and to visually monitor the effect of the desilication treatments. In Figure 4(a) a SEM image of the parent sample is shown. It can be seen that the crystals

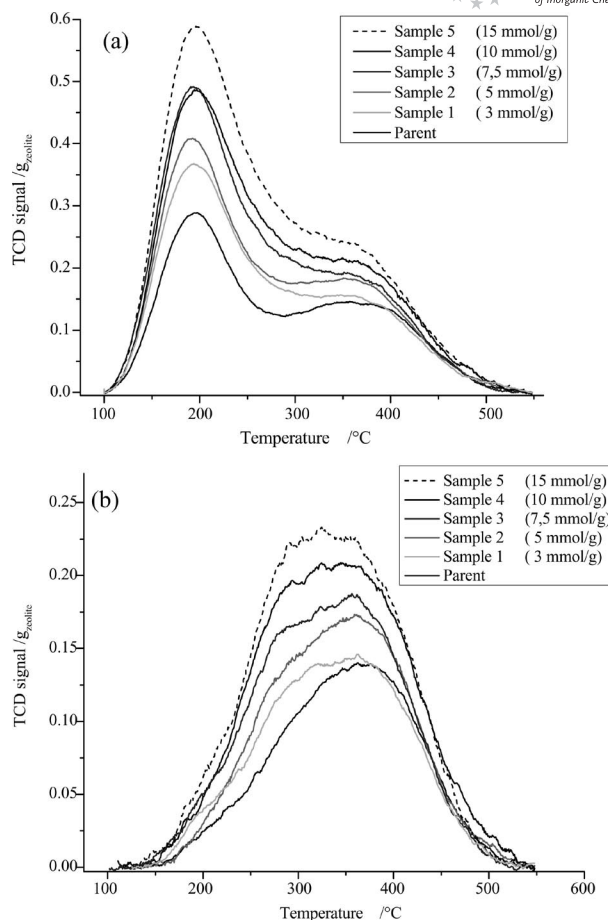


Figure 3. NH_3 desorption curves of parent sample and samples 1–5. Weakly bound NH_3 desorbed in He at (a) 100 °C for 1 h and (b) at 175 °C desorbing for 2 h.

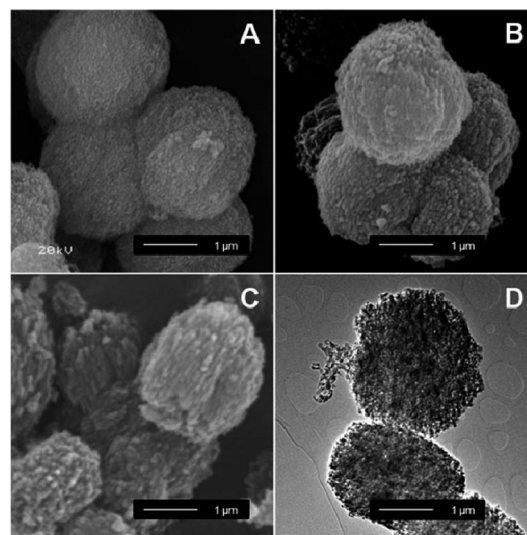


Figure 4. (a)–(c) SEM images of the parent sample, sample 7 (desilicated 10 min.) and sample 10 (desilicated 30 min), respectively. (d) TEM image of sample 10 (desilicated 30 min).

exhibit the well-known sponge-like morphology characteristic of mesoporous carbon-templated MFI zeolites.^[34] Overview images of the parent sample confirmed that the crystals were similar in size (2–3 μm long) and that the vast majority of them exhibited this morphology. Figures 4(b) and (c) show SEM images of desilicated samples obtained after 10 min (sample 7) and 30 min (sample 10) treatment times, respectively. From these images, it is evident that desilication leads to a gradual “roughening” of the crystals, which appear to be more and more rugged as the desilication time is increased. TEM analyses also revealed the sponge-like morphology of the crystals as evident from the highly contrasted image of the 30 min desilicated samples shown in Figure 4(d).

Conclusions

We have shown that the porosity of carbon-templated mesoporous ZSM-5 may be enhanced by a factor of at least two by desilication of such a sample in terms of mesopore surface area as well as mesopore volume. Two types of desilication protocols were applied for tuning the porosity of the carbon-templated mesoporous sample: variation in the volume of hydroxide solution and variation in reaction time. Pore-size distribution plots revealed that at lower desilication strengths both newly generated smaller mesopores (initially centered below 10 nm) as well as mesopores already present in the sample (centered around ca. 20–30 nm) contributed to the mesopore volume. With increased desilication strength, these smaller mesopores grew larger, eventually, after excessive desilication, into the macropore region. The method applied here could easily be extended to other zeolite structure types, and it therefore provides a useful and easy approach for systematically generating highly mesoporous zeolite samples.

Experimental Section

A mesoporous ZSM-5 sample was prepared by carbon-templating according to a modified literature procedure.^[35] A nominal Si/Al ratio of 45 was used in the gel. Briefly, 2 g of carbon black pearls 2000 was impregnated with a fresh solution of aluminium isopropoxide in tetrahydrofuran (0.084 g in 6 mL) and left to dry overnight. Then the carbonaceous material was impregnated with a mixture of tetrapropylammonium hydroxide (3.44 g, 40 wt.-%), aqueous sodium hydroxide (0.1 g in 0.5 g H_2O) and ethanol (3.03 g), and left to dry overnight. The material was impregnated with tetraethyl orthosilicate (3.87 g) and left to dry overnight before being crystallized at 180 °C for 5 d. The carbon matrix was removed by calcination at 550 °C in static air for 20 h reached at a ramp of ca. 2 °C/min. The proton form of the zeolites was obtained by threefold ion-exchange in a 1 M NH_4NO_3 solution and calcination at 550 °C in static air for 4 h. The sample was subjected to different desilication procedures by immersion of the zeolite samples in aqueous sodium hydroxide solutions at 65 °C for various periods of time. After reaction, the desilicated samples were collected by filtration and washed thoroughly with water. Nitrogen physisorption measurements were conducted with a micromeritics ASAP 2020. Powder X-ray diffraction (XRD) patterns of the par-

ent and desilicated samples were recorded with a Bruker AXS powder diffractometer. Scanning electron micrographs (SEM) were recorded with a JEOL JSM 5900 equipped with an LaB_6 filament. Prior to measurements, the samples were sputter-coated with Au for 40 s by using a Polaron SC 7620. Transmission electron microscopy (TEM) images and selected area diffraction (SAD) were recorded with a JEM 2000 FX with an accelerating voltage of 300 kV, as described previously.^[36] NH_3 -TPD measurements were performed with a Micromeritics Autochem II equipped with a TCD detector. Samples were transformed into proton form prior to NH_3 -TPD analysis through a similar procedure as described above for the parent material. Dry weight of the samples was found after evacuation at 300 °C for 1 h. Weakly bound ammonia was desorbed prior to measurement at 100 °C in an He flow of 25 mL/min for 1 h or at 175 °C in an He flow of 50 mL/min for 2 h, respectively.

Supporting Information (see footnote on the first page of this article): N_2 physisorption isotherms and crystal-size measurements (calculated by use of the Scherrer equation from X-ray data).

Acknowledgments

The Center for Sustainable and Green Chemistry is sponsored by the Danish National Research Foundation. The authors thank Bodil F. Holten for technical assistance.

- [1] A. Corma, *Chem. Rev.* **1995**, 95, 559.
- [2] A. Corma, *Chem. Rev.* **1997**, 97, 2373.
- [3] M. Hartmann, *Angew. Chem. Int. Ed.* **2004**, 43, 5880.
- [4] Y. Tao, H. Kanoh, L. Abrams, K. Kaneko, *Chem. Rev.* **2006**, 106, 896.
- [5] J. C. Groen, C. H. Christensen, K. Egeblad, C. H. Christensen, J. Pérez-Ramírez, *Chem. Soc. Rev.* **2008**, accepted.
- [6] M. E. Davis, C. Saldarriaga, C. Montes, J. Garces, C. Crowder, *Nature* **1988**, 331, 698.
- [7] C. C. Freyhard, M. Tsapatsis, R. F. Lobo, K. J. Balkus, *Nature* **1996**, 381, 295.
- [8] T. Wessels, C. Baerlocher, L. B. McCusker, E. J. Croyghton, *J. Am. Chem. Soc.* **1999**, 121, 6242.
- [9] A. Corma, M. Diaz-Cabanas, J. Martinez-Triguero, F. Rey, J. Rius, *Nature* **1992**, 418, 514.
- [10] L. Tosheva, V. P. Valtchev, *Chem. Mater.* **2005**, 17, 2494.
- [11] P. A. Jacobs, E. G. Derouane, J. Weitkamp, *J. Chem. Soc., Chem. Commun.* **1981**, 591.
- [12] M. A. Camblor, A. Corma, S. Valencia, *Microporous Mesoporous Mater.* **1998**, 25, 59.
- [13] C. Madsen, C. J. H. Jacobsen, *Chem. Commun.* **1999**, 673.
- [14] W.-C. Li, A.-H. Lu, R. Palkovits, W. Schmidt, B. Spliethoff, F. Schüth, *J. Am. Chem. Soc.* **2005**, 127, 12595.
- [15] C. J. H. Jacobsen, C. Madsen, J. Houzvicka, I. Schmidt, A. Carlsson, *J. Am. Chem. Soc.* **2000**, 122, 7116.
- [16] M. Ogura, S. H. Shinomiya, J. Tateno, Y. Nara, E. Kikuchi, M. Matsukata, *Chem. Lett.* **2000**, 882.
- [17] F.-S. Xiao, L. Wang, C. Yin, K. Lin, Y. Di, J. Li, R. Xu, D. S. Su, R. Schlögl, T. Yokoi, T. Tatsumi, *Angew. Chem. Int. Ed.* **2006**, 45, 3090.
- [18] H. Wang, T. Pinnavaia, *Angew. Chem. Int. Ed.* **2006**, 45, 7603.
- [19] K. Egeblad, C. H. Christensen, M. Kustova, C. H. Christensen, *Chem. Mater.* **2008**, 20, 946.
- [20] K. Egeblad, C. H. Christensen, M. Kustova, C. H. Christensen, “Mesoporous Zeolite Crystals”, in *Zeolites: From Model Materials to Industrial Catalysts* (Eds.: J. Cejka, J. Perez-Pariente, W. J. Roth), Transworld Research Network, Kerala, India, **2008**, pp. 391–442.
- [21] M. Y. Kustova, P. Hasselriis, C. H. Christensen, *Catal. Lett.* **2004**, 96, 205.

- [22] X. Wei, P. G. Smirniotis, *Microporous Mesoporous Mater.* **2005**, 89, 170.
- [23] Y. Tao, H. Kanoh, K. Kaneko, *J. Phys. Chem. B* **2003**, 107, 10974.
- [24] J. C. Groen, L. A. A. Peffer, J. A. Moulijn, J. Pérez-Ramírez, *Chem. Eur. J.* **2005**, 11, 4983.
- [25] J. C. Groen, J. A. Moulijn, J. Pérez-Ramírez, *J. Mater. Chem.* **2006**, 16, 2121.
- [26] M. Bjørgen, F. Joensen, M. S. Holm, U. Olsbye, K.-P. Lillerud, S. Svelle, *Appl. Catal. A* **2008**, 345, 43.
- [27] Y. Tao, H. Kanoh, K. Kaneko, *Adsorption* **2006**, 12, 309.
- [28] Y. H. Chou, C. S. Cundy, A. A. Garforth, V. L. Zholobenko, *Microporous Mesoporous Mater.* **2006**, 89, 78.
- [29] J. C. Groen, L. A. A. Peffer, J. A. Moulijn, J. Pérez-Ramírez, *Colloids Surf., A* **2004**, 241, 53.
- [30] J. C. Groen, W. Zhu, S. Brouwer, S. J. Huynink, F. Kapteijn, J. A. Moulijn, J. Pérez-Ramírez, *J. Am. Chem. Soc.* **2007**, 129, 355.
- [31] M. Ogura, S. Shinomiya, J. Tateno, M. Nomura, E. Kikuchi, M. Matsukata, *Appl. Catal. A* **2001**, 219, 33.
- [32] Y. Song, X. Zhu, T. Song, Q. Wang, L. Xu, *Appl. Catal. A* **2006**, 302, 69.
- [33] J. S. Jung, J. W. Park, G. Seo, *Appl. Catal. A* **2005**, 288, 149.
- [34] K. Zhu, K. Egeblad, C. H. Christensen, *Eur. J. Inorg. Chem.* **2007**, 3955.
- [35] M. Y. Kustova, A. L. Kustov, C. H. Christensen, *Stud. Surf. Sci. Catal.* **2005**, 158, 255.
- [36] K. Egeblad, M. Kustova, S. K. Klitgaard, K. Zhu, C. H. Christensen, *Microporous Mesoporous Mater.* **2007**, 101, 214.

Received: August 5, 2008

Published Online: October 22, 2008